Thermal, thermo-oxidative and thermomechanical degradation of PLA: a comparative study based on rheological, chemical and thermal properties

A.A. Cuadri *, J.E. Martín-Alfonso

Departamento de Ingeniería Química, Centro de Investigación en Tecnología de Productos y Procesos Químicos (Pro^{2}TecS), Campus de 'El Carmen', Universidad de Huelva, 21071, Huelva (Spain).

* Author to whom correspondence should be addressed:

A.A. Cuadri

E-mail: antonio.cuadri@diq.uhu.es

Phone: +34 959 21 98 82

Fax: +34 959 21 93 85

ABSTRACT

This research studies the effect of thermal, thermo-oxidative and thermomechanical degradation conditions on the melt rheological, chemical and thermal properties of PLA at temperatures around its normal processing temperature. Thermal and thermo-oxidative degradations were conducted on a rheometer by using nitrogen or air as gas, respectively, and the thermomechanical degradation was performed on a mixer equipped with two counter-rotating rollers. Dynamic oscillatory rheology, TGA, DSC and FTIR were performed on PLA samples subjected to different degradation conditions: temperature (180, 200 or 220 ºC), time (15, 30 or 60 min), atmosphere (air or atmosphere) and the application of mechanical stress or not. Thus, rheological results indicate the synergic effect that temperature, mechanical stress and time exerts on the extent of chain scission phenomena, which was also corroborated by FTIR results; however, the individual contribution of mechanical stress diminishes gradually with the degradation time, being more pronounced for higher degradation temperature. In addition, degree of crystallinity (χ_c) turned out not to be a suitable parameter for comparing degraded samples, since all of them became amorphous after degradation. Instead, glass transition (T_g) and cold crystallization (T_{cc}) temperatures as well as the cold crystallization enthalpy (ΔH_{cc}) reveal that the chain scission phenomena makes degraded samples easier to crystallize. Finally, TGA results point out a worsening of the PLA thermal stability, with lower values of the characteristic temperatures ($T_{5\%}$ and T_{max}) for degraded samples.

Keywords: Poly(lactic acid), thermal degradation, thermo-oxidative degradation, thermomechanical degradation, dynamic oscillatory rheology.

1. INTRODUCTION

Poly(lactic acid) (PLA) is an emerging polymer from renewable sources having good thermoplastic behaviour, good processability and fulfilling biodegradable requirements. These properties make it a promising candidate to replace petroleum-based polymers like polyolefins in different industrial applications (e.g., packaging, films for agro-industry, fibers, etc.) [1-5]. In addition, PLA can be found under several forms depending on the enantiomeric ratio of the lactic acid group, namely PLLA (poly-L-lactic acid), PDLA (poly-D-lactic acid) and the common one, PDLLA (poly-DL-lactic acid), each PLA having specific properties [4].

Likewise many aliphatic polyesters, PLA is reported to degrade during processing due to the action of external driving force (e.g., temperature, oxygen, mechanical stress, etc.) [2]. Thus, depending on their combination, different polymer degradation can occur: thermal degradation (i.e., polymer degradation only due to the effect of temperature), thermo-oxidative degradation (i.e., degradation arises as a result of elevated temperatures and the presence of oxygen) and thermomechanical degradation (i.e., when also mechanical stress is involved) [6,7]. Regarding PLA, its thermo-oxidative degradation at the normal processing temperature (around 200 ºC) follows a random chain scissions mechanism determining a significant level of molecular degradation and leading to the formation of degradation products (e.g., linear hydroxyl, ester and carbonyl groups, etc.) [1,8]. This is all reflected in a dramatic change of the molecular structure, typically evolve towards a decrease in the molecular weight, which are undesired, not only because the material's melt viscosity and elasticity decrease, but also the processing equipment can be damaged due to the volatile lactide formation [2,5,7,9].

On these grounds, some authors [4,5,10] reported studies about both thermo-oxidative

and thermomechanical degradation of PLA and PLA-based composites, but at temperatures below PLA's melting point. However, since the main production processes of PLA are based on melt processing, especially extrusion and injection moulding which require high temperature and mechanical stress, it is crucial to understand the structural, thermal and rheological changes that can occur during their processability [3]. Interestingly, no studies were found in the scientific literature studying the effect that temperature, time, mechanical stress and atmosphere exert on melt rheological response, chemical and thermal properties of virgin PLA at temperatures around its processing temperatures (~ 200 ºC).

In order to detect and quantify the changes in chemical structure of polymer macromolecules, dynamic oscillatory rheology of melted polymers, especially under low frequency, was found to be one of the most efficient techniques for detecting microstructural transformations due to chain scission and long chain branching/crosslinking, because different polymer chains could behave diagnostic viscoelastic response in long time regime due to the difference of relaxation rate [11-14]. In addition to that, dynamic oscillatory rheological measurements are conducted in the linear viscoelasticity (LVE) region, so its strain is too small to damage the structure of a polymer, in contrast with the large strains applied for the steady shear measurements [11,15].

Therefore, the objective of this contribution is to investigate the effect that thermal, thermo-oxidative and thermomechanical degradation conditions (which are the results of combining different atmosphere, degradation time/temperature and mechanical stress) exert on the melt rheological response, chemical and thermal properties of virgin PLA at temperature around its normal processing temperature (200 ºC). To that end, thermal and thermo-oxidative degradations were conducted on a rheometer under

nitrogen or air atmosphere, respectively, and the thermomechanical degradation was performed on a mixer equipped with two counter-rotating rollers. Melt rheological behaviour was studied by means of dynamic oscillatory measurements, and the chemical and thermal changes due to the degradations were evaluated by thermogravimetric analysis, differential scanning calorimetry and Fourier transform infrared spectroscopy.

2. MATERIAL AND METHODS

2.1. Material and sample preparation

The poly(DL-lactide) (PDLLA) used in this study was kindly supplied by NatureWorks (USA). The selected grade 2002D had a D content of 4.25 %, $M_w = 2.09 \cdot 10^5$ g mol^{-1}, $M_n = 1.01 \cdot 10^4$ g mol^{-1} and $M_w/M_n = 2.07$.

Prior to use, PLA pellets were dried in an oven for 2 h at 100 ºC for preventing hydrolysis of PLA since this polymer is very hygroscopic. Before its thermal or thermo-oxidative degradations, PLA disks about 1.5 mm in thickness and 25 mm in diameter were prepared by compression-moulding in a hot press. To that end, firstly, as-received PLA pellets were subjected to 50 bar of pressure for 5 min, at 175 ºC. Subsequently, the disks were allowed to cool down to room temperature. These conditions (50 bar, 175 ºC, 5 min) were selected to diminish to the maximum a possible polymer degradation during the compression-moulding, since the objective of this stage was only to obtain disk-shaped specimens.

2.2. Thermal/thermo-oxidative degradation and rheological characterization

Rheological measurements were carried out in a controlled-stress rheometer Physica MCR-301 (Anton Paar, Austria), using rough plate-and-plate geometry (25 mm diameter; 1 mm gap), and equipped with a CTD450 convection oven, which provides a gas flow of 1 L/min. Before starting with the rheological measurements (stress or

frequency sweep test), the thermal or thermo-oxidative degradation of PLA was conducted on the rheometer itself, by using nitrogen or air, respectively, as gas. The procedure can be summarized as follows: a) a PLA disk was placed on the lower plate at the degradation temperature (180, 200 or 220 ºC); b) after 30 s, which was used to ensure that the sample is in melt state, the gap was adjusted to 1 mm and the remaining melted PLA was trimmed with the help of a metallic spatula. Afterwards, the convection oven was closed; c) the sample was degraded at the previously selected degradation temperature for 0, 15, 30 or 60 min under nitrogen or air atmosphere; d) a stress sweep tests, at 1 rad/s, was performed to determine the LVE region; e) a fresh PLA disk was again subjected to the same degradation conditions (i.e., the steps a), b) and c) were repeated) and a frequency sweep test, from 100 to 0.1 rad/s, under a stress value within the LVE region, was performed. It is important to highlight that both stress and frequency sweep tests were always conducted under nitrogen atmosphere for avoiding further degradation during the testing time.

On the other hand, after completing the step b) (i.e., just before starting PLA degradation), a time sweep test (within the LVE region) was performed for 60 min at each degradation temperature (180, 200 or 220 ºC) and under nitrogen or air atmosphere. This enables us to monitory the evolution of the linear viscoelastic functions with the degradation time for samples degraded under different atmospheres. Consequently, for time sweep tests, the testing time corresponds to the degradation time.

2.3. Thermomechanical degradation

The thermomechanical degradation was carried out in a Rheomix 3000p mixer from Thermo Haake (Germany), equipped with two counter-rotating rollers. The rotor speed was 50 rpm and the set temperature, similar to the thermal/thermo-oxidative

degradation, was 180, 200 or 220 ºC. After 15, 30 or 60 min of mixing the sample was removed and stored at room temperature until its characterization. A portion was used for its rheological characterization with the controlled-stress rheometer Physica MCR-301. In this case, after completing the stages a) and b) above-commented, the stress and frequency sweep tests were conducted at the same degradation temperature applied in the mixer (and also under nitrogen atmosphere).

2.4. Thermal and chemical characterization

In addition to rheological characterization, thermogravimetric (TGA) analysis, differential scanning calorimetric (DSC) tests and a chemical characterization by Fourier transform infrared spectroscopy (FTIR) were carried out on dried PLA and its corresponding degraded samples. These samples were directly taken from the rheometer when the frequency sweep test is finished (for the thermal or thermo-oxidative degradation) or from the mixer (for the thermomechanical degradation).

TGA analysis were conducted in a TA Q-50 (TA Instrument, USA). Temperature sweeps (10 ºC/min; between 30 and 600 ºC) were carried out on 5–10 mg samples placed on a Pt pan and under nitrogen gas flow of 100 mL/min. The temperature corresponding to a 5 wt. % weight loss ($T_{5\%}$) and the temperature at which decomposition rate is maximum (T_{max}) were obtained from TGA curves.

DSC tests were performed with a TA Q-100 (TA Instruments, USA) using 5–10 mg samples sealed in hermetic aluminium pans. All tests were performed with a nitrogen gas flow rate of 50 mL/min. The samples were subjected to two heating steps, from 0 to 200 ºC, and an intermediate cooling step, all them at the same rate of 10 ºC/min. The objective of the first heating step was to eliminate the heat history of the sample. Therefore, the glass transition (T_g), cold crystallization (T_{cc}) and melting (T_m) temperatures, and the cold crystallization (ΔH_{cc}) and melting (ΔH_m) enthalpies, were

169 recorded from the second heating sequence.

170 FTIR spectra were recorded in a Jasco FT/IR 4200 spectrometer (Jasco Analytical
171 Instrument, Japan), in a wavenumber range of 400-4000 cm^{-1}, at 4 cm^{-1} resolution in the
172 absorbance mode. FTIR analysis was carried out on films of dried PLA and its
173 corresponding degraded samples. Surface IR analyses of the films were conducted using
174 ATR accessory fitted with a diamond crystal. For film preparation, 4 mg of each sample
175 was dissolved in 4 mL of dichloromethane, the solution was transferred to a Petri dish
176 and, after solvent evaporation, a thin film was obtained [16].

177 In order to ensure accurate results, at least three replicates were conducted for every
178 sample/test. Figures present the average values and the data were presented as mean ±
179 standard deviation (SD).

180 **3. RESULTS AND DISCUSSION**

181 **3.1. Melt rheological properties**

182 Figure 1 displays the evolution of the storage (G') and loss (G'') modulus with the
183 degradation time for samples subjected to different degradation temperatures (180, 200
184 and 220 ºC) under nitrogen (thermal degradation) or air (thermo-oxidative degradation)
185 atmosphere. As can be observed, all degraded PLA samples, regardless of the
186 degradation temperature and atmosphere, show a predominant viscous behaviour, with
187 G'' values higher than G' over the entire degradation time. Interestingly, significant
188 differences can be deduced by comparing the results obtained after degradation under
189 nitrogen or air atmosphere. On the one hand, for each degradation temperature, the
190 values of both moduli for the thermal degradation samples (i.e., samples degraded under
191 nitrogen atmosphere) remain constant with the time. These results confirm that 30 s is
192 enough waiting time before starting the rheological tests, since no decrease of both
193 moduli are noticed and, consequently, the sample is completely melted after this waiting

194 time. In addition to that, under nitrogen atmosphere, an increase in the degradation
195 temperature is reflected in lower G' and G'' values. This fact points out that a
196 degradation temperature increase brings an acceleration in chain scission phenomena
197 [12,17-19]. On the other hand, under air atmosphere (i.e., thermo-oxidative
198 degradation), degraded PLA samples show similar qualitative response for each
199 degradation temperature. When increasing the degradation time, both moduli undergo a
200 drop, which is more remarkable for the first 15 min, and then they tend to level off.
201 These facts can be more easily observed for those samples degraded at higher
202 temperatures, in particular for that degraded at 220 ºC (Figure 1C). Furthermore, two
203 consequences can be deduced from the thermo-oxidative degradation: a) when
204 increasing degradation time, the difference between both moduli is kept almost
205 constant, which implies that the predominant viscous behaviour is maintained, and b)
206 the isothermal frequency sweep tests should be conducted under nitrogen atmosphere,
207 in order to prevent PLA degradation during its testing time (ca. 14 min).
208 It is well known that the dynamic oscillatory measurements are very sensitive to the
209 topological structure changes of melted polymers as a consequence of alterations in its
210 molecular weight, distribution (polydispersity) and level of long chain branching [12,17,
211 18,20,21]. After studying the evolution of linear viscoelastic functions with the
212 degradation time for thermal and thermo-oxidative degradation (i.e., degradation under
213 nitrogen or air atmosphere), the interest is now focused on making a comparative study
214 about the changes on melt rheological properties for all the degradation procedure here
215 proposed. This involves comparing PLA samples after being degraded in the rheometer
216 under nitrogen (thermal degradation) or air (thermo-oxidative degradation) atmosphere,
217 together with those from the mixer (thermomechanical degradation). To that end,

218 frequency sweep tests were conducted on these samples at the same time/temperature
219 degradation.
220 As an illustrative example, the evolution of both viscoelastic moduli and complex
221 viscosity (|η*|) with frequency are displayed in Figure 2A and 2B, respectively, after
222 subjecting PLA sample to different degradation times (from 0 to 60 min) at 180 ºC
223 under air atmosphere. From Figure 2A, it is deduced that degraded samples show
224 similar mechanical spectra, which are characterized by a predominant viscous behaviour
225 (G''>G'), typical of the terminal zone reported for polymer [22]. In addition, as
226 expected from Figure 1A, when increasing degradation time, both moduli decreases,
227 especially after 15 min of degradation. Regarding the |η*| in Figure 2B, all samples
228 present a Newtonian region at low frequencies, which is characterized by a constant
229 viscosity (η_0), followed by a shear-shinning drop beyond a threshold (or "critical")
230 value of frequency. All degraded samples here studied (after thermal, thermo-oxidative
231 or thermomechanical degradation) present similar mechanical spectrum, which is the
232 typical response for linear PLA [23-26].
233 Some researchers [12,17,18,20,21] have reported the significance of the |η*| vs. ω curve
234 for understanding possible changes in the length and level of entanglement of polymer
235 chains. They stated that: a) an increase in |η*| at low/intermediate frequencies is related
236 to a drop in the chain mobility which may result from chain branching, and b) a
237 decrease in η_0 values indicates that chain scission may have occurred. On these grounds,
238 the increase in |η*| observed for the thermo-oxidative degradation of HDPE was
239 ascribed to an increase in the long chain branching/crosslinking phenomena [19].
240 However, as for PLA, it can be deduced from Figure 2B that an increase of degradation
241 time favours the chain scission phenomena and an earlier decrease of η_0. In this sense,

the η_0 values from Figure 2B can be used to estimate their corresponding weight-average molecular weights (M_w) by the following equation [27]:

$$\eta_0 = 5.50 \cdot 10^{-15} M_W^{3.4} \qquad (1)$$

Thus, for the PLA samples subjected to thermo-oxidative included in Figure 2B, the M_w values decreased from $1.33 \cdot 10^5$, $1.03 \cdot 10^5$, $9.40 \cdot 10^4$ to $8.58 \cdot 10^4$ after 0, 15, 30 and 60 min of degradation time, respectively. Similarly, a decrease in η_o values after subjecting PLA samples to thermo-mechanical degradation shall be accompanied by lower M_w values, again due to the chain scission phenomena.

In addition to that, the linear viscoelasticity functions (G' and G'') from Figure 2A can be used to obtain the relaxation behaviour, which provides valuable information about possible changes in PLA structures due to branching or chain scission phenomena [28]. A discrete relaxation spectrum may be described by many Maxwell elements combined in series, the generalized Maxwell model. Thus, both moduli for a generalized Maxwell model are given for the following relationships [22,29]:

$$G'(\omega) = \sum_{i=1}^{N} G_i \frac{(\omega\lambda_i)^2}{1 + (\omega\lambda_i)^2} \qquad (2)$$

$$G''(\omega) = \sum_{i=1}^{N} G_i \frac{\omega\lambda_i}{1 + (\omega\lambda_i)^2} \qquad (3)$$

where G_i and λ_i are the relaxation strength and relaxation time, respectively, and the sets of G_i and λ_i represent the discrete Maxwell relaxation time spectrum. In this paper, the discrete relaxation spectrum (Gi vs. λi) was calculated by means of a linear regression procedure using algorithms developed in MathCad v14 Pro software. It was corroborated that for the experimental frequency range used in Figure 2 (from 0.1 to 100 rad/s) four Maxwell elements are sufficient for recalculated the values of G' and G'' with high levels of significance. Figure 3 shows the discrete relaxation spectrum for

the samples included in Figure 2B (i.e., those samples subjected to thermo-oxidative degradation and different degradation times), which are similar to those reported by Wang et al. [28] for a similar frequency range. The presence of long, heavy and branched PLA chains restricts their mobility which is reflected in an increase in the relaxation time. However, in our case, as the chain scission phenomena increases with the degradation time, the resulting short PLA chains lead to lower relaxation times [30]. Finally, the discrete relaxation spectrum gathered in Figure 3 can be also combined for determining η_o values as follows [29]:

$$\eta_0 = \sum_{i=1}^{N} G_i \lambda_i \qquad (4)$$

Interestingly, η_o values of values 1609, 654, 483 and 364 Pa·s were calculated using the equation (5) which are in good agreement with those displayed in Figure 2B, indicating that the procedure to obtain the discrete relaxation spectra were appropriate.

Taking account that all degraded samples present a $|\eta^*|$ vs. ω curve similar to that displayed in Figure 2B, the estimation of a relative modification index (R.M.I.) from the values of η_0 may be considered as a useful parameter to quantify the chain scission achieved after PLA degradation. Thus, a R.M.I. for each degradation temperature (180, 200 and 220 ºC) has been defined as follows:

$$\text{R.M.I.} = \frac{\eta_{0,t=0}}{\eta_{0,t}} \qquad (5)$$

where $\eta_{0,t=0}$ and $\eta_{0,t}$ are the complex viscosity value at 0.1 rad/s for a sample subjected to a degradation time of 0 min (i.e., just after 30 s of waiting time before testing) and after a time "t" of 15, 30 or 60 min of degradation, both at the same degradation temperature. The values of $\eta_{0,t=0}$ are 1429, 451 and 134 Pa·s for degradation temperatures of 180, 200 and 220 ºC, respectively.

Hence, this parameter allows us to quantify the drop in melt viscosity due to the chain scission for the different degradation conditions applied, as well as the individual contribution of temperature or stress. Thus, for the same degradation temperature, higher R.M.I. values would indicate that the chain scission mechanism has taken place in a greater extent. Figure 4 displays the evolution of the R.M.I. with the degradation time after thermal, thermo-oxidative and thermomechanical degradation at the three degradation temperatures considered in this work. Firstly, as no change in G' and G'' with the time are noticed for the degradation under nitrogen atmosphere (Figure 1), R.M.I. takes a value of 1 for each temperature. As for thermo-oxidative degradations (i.e., those conducted under air atmosphere) significant conclusions may be deduced: a) on the one hand, for each temperature, when the degradation time increases, so does its corresponding R.M.I. values and, b) on the other hand, for a fixed degradation time, higher R.M.I. values are obtained as degradation temperature rises, mainly for those degraded at 220 ºC. Regarding the thermomechanical degradations, their R.M.I. values displayed in Figure 4 are the contribution of the effect of both temperature and stress applied in the mixer. Therefore, if the R.M.I. values of the thermo-oxidative degradation (which are only due to the temperature) are subtracted from those obtained from thermomechanical degradation, it can be stated that the individual contribution of mechanical stress diminishes gradually with the degradation time, being more pronounced for higher degradation temperature.

In any case, these results confirm the synergic effect that temperature, mechanical stress and time exerts on the chain scission, which are consequence of the PLA degradation mechanism. McNeill and Leiper [31] reported their findings after PLA degradation under inert atmosphere without being subjected to any mechanical stress. Thus, PLA thermal degradation occur predominantly by random chain scissions through non-

312 radical reactions along the polymer backdone. Depending of the point in the backbone
313 at which this reaction occurs, the final product could be a lactide molecule, an
314 oligomeric ring with more than two repeat units or acetaldehyde plus carbon monoxide.
315 Therefore, all these reactions lead to a reduction of molecular weight, which is reflected
316 in lower melt viscosity values. In addition, the presence of oxygen under the PLA
317 thermo-oxidative degradation induces a chain scission mechanism of alkoxyl radicals
318 (alkyl- and acyl-oxygen), thus leading the formation of new free radicals that can cause
319 chain scission [1,8,16] and the formation of oxidation product degradations (mainly
320 ester and carbonyl groups). Finally, the high level of stress applied in the mixer
321 produces a decrease in the carbon-oxygen bonding energy and alkyl and acyl-oxygen
322 homolysis on the backbone of PLA and, consequently, this fact again favours the chain
323 scission which is noticed in higher values of R.M.I. [1,4,8,10,16]. The McNeill and
324 Leiper work supports that radical reaction just occurs at temperature above 270 ºC.
325 However, although the temperature degradation used in the present work was lower
326 than that, it has been demonstrated that such reactions might occur due to the high level
327 of stress and the oxygen presence inside the mixer [5,16].

328 **3.2. Chemical and thermal properties**

329 Once the melt rheological properties of PLA samples subjected to different degradation
330 conditions has been studied, the objective now is to deepen their effects on the chemical
331 structure and thermal properties. To that end, Fourier transform infrared spectroscopy
332 (FTIR), differential scanning calorimetric (DSC) and thermogravimetric (TGA) analysis
333 were conducted on degraded PLA at 200 ºC (since this temperature represents a
334 potential temperature in the perspective of extrusion process).

335 Assessment of the chemical structure changes of degraded PLA samples provoked by
336 the degradation conditions applied were investigated by infrared analysis. Figure 5

337 displays the ATR-FTIR spectra in the range of 2000 to 600 cm^{-1} for virgin PLA as well
338 as selected degraded samples after two degradation times (15 min or 60 min) and
339 subjected to thermo-oxidative degradation (referred to as "PLA,15min,TO" and
340 "PLA,60min,TO") or thermomechanical degradation ("PLA,15min,TM" and
341 "PLA,60min,TM"). The spectrum for degraded sample after thermal degradation for 15
342 min ("PLA,15min,T") is coincident with that after 60 min of degradation and,
343 consequently, it is not included for the sake of comparison.
344 It is well known that the random chain scission reaction associated with the formation
345 of anhydrides, carbonyl and/or carboxyl groups, is the predominant degradation
346 pathway for PLA during its photo-oxidation (with UV light irradiation) and thermo-
347 oxidative/thermomechanical degradation. As a consequence, the most noticeable
348 changes appear at 1085 and 1183 cm^{-1} due to the asymmetric vibration of the ester
349 group, and at 1750 cm^{-1} attributed to the carbonyl stretching [4,5,10,16,32,33]. In
350 addition, all degraded PLA samples (including those obtained under nitrogen
351 atmosphere) present changes in their spectra in the 750 to 650 cm^{-1} which is assigned to
352 changes in crystallinity [34].
353 Aiming to obtain comparable results without the experimental influence, absorbance
354 values of these characteristic peaks (at 1750, 1183 and 1083 cm^{-1}) were normalized
355 using the absorbance value at 1455 cm^{-1} assigned to the asymmetric bending of CH_3
356 group and known to be a suitable as internal standard for PLA [4,5,10,16]. Thus, the
357 absorbance ratios displayed in the Figure 6 provide valuable information about the
358 chemical changes due to the different degradation conditions applied. As can be
359 deduced, no significant changes are noticed on those samples subjected to thermal
360 degradation, which points out that nitrogen is required to prevent the PLA chain
361 scission phenomena with the degradation time. However, after expose to thermo-

362 oxidative or thermomechanical degradation conditions, the absorbance ratio clearly
363 increases with the degradation time rises, especially for the formation the new carbonyl
364 compounds (at 1750 cm^{-1}). These results are in agreement with the R.M.I. displayed in
365 Figure 4, indicating, again, the synergic effect that degradation time and stress exerts on
366 the extent of the PLA chain scission at 200 ºC.
367 DSC analysis was carried out in an attempt to find out possible changes of PLA thermal
368 events induced by the degradation conditions applied. Figure 7 shows the DSC
369 thermograms derived from the second heating scan of virgin PLA and selected degraded
370 samples, and in Table 1, the corresponding glass transition (T_g), cold crystallization
371 (T_{cc}) and melting (T_m) temperatures, and crystallization (ΔH_{cc}) and melting (ΔH_m)
372 enthalpies are summarized. In addition, degree of crystallinity (χ_c) in each sample was
373 calculated as follows:

374 $$\chi_c(\%) = \frac{\Delta H_m - \Delta H_{cc}}{\Delta H_m^{100\%}} \cdot 100 \qquad (6)$$

375 where $\Delta H_m^{100\%}$ is the theoretical melting enthalpy for PLA with 100 % of crystallinity.
376 According to the literature [35], a theoretical enthalpy of 93.1 J/g was used for the
377 melting enthalpy of PLA with 100 % of crystallinity.
378 It can be observed that virgin PLA only presents a thermal event at around 59 ºC which
379 corresponds to the glass transition of its amorphous fraction. Thus, only the first heating
380 ramp (data no shown) shows, at about 148 ºC, the melting peak of the PLA crystalline
381 fraction. The absence of the melting peak for the second heating ramp indicates that
382 recrystallization upon cooling from the melt does not occur at the cooling rate of 10
383 ºC/min applied (too fast for the PLA polymer chains to reorganize into crystalline
384 regions). Taking the melting enthalpy from the first heating ramp, virgin PLA displays a
385 percentage of crystallinity of 34.3 %. Interestingly, all degraded samples present,

386 besides the glass transition and melting peak above-commented, a new cold
387 crystallization peak which extents in different temperature range depending on the
388 degradation procedure (i.e., thermal, thermo-oxidative or thermomechanical) applied.
389 As reported Signori et al. [2], when PLA is degraded at 200 ºC and under nitrogen
390 atmosphere the cold crystallization is also noticed. Even though no significant
391 differences on T_g values are noticed between thermo-oxidative and thermomechanical
392 degraded samples, all these systems display a significant decrease in T_g value compared
393 to virgin PLA, which can be attributed without any doubt to the chain scission process
394 occurring during their degradation [4,10]; however, thermal degraded samples (under
395 nitrogen atmosphere) present a similar value, since chain scission phenomena is not
396 relevant.
397 If attention is paid on the crystallinity degree (χ_c), all degraded samples are amorphous
398 (crystallinity degree is about zero), since the absolute values of the cold crystallization
399 and melting enthalpy are almost the same due to the slow crystallization kinetics of
400 PLA and the relatively fast cooling rate applied (10 ºC/min). Therefore, χ_c is not a
401 suitable parameter for studying the effect of degradation conditions.
402 On the other hand, it is possible to observe that thermograms of degraded samples after
403 thermo-oxidative degradation (PLA,15min,TO and PLA,60min,TO), and more
404 pronounced for that subjected to thermomechanical degradation at the longest time
405 (PLA,60min,TM), show a double melting peak attributed to the melting crystalline
406 phases formed during the second heating ramp, since no crystallization is negligible
407 during the cooling cycle. It is well known [10,36-38] that PLA exhibits double melting
408 behaviour associated to with the stable pseudo-orthorhombic structure melting at the
409 higher temperature (α-form) and the orthorhombic (β-form) that melts at a lower
410 temperatures. In addition, both characteristic melting temperatures for the

411 thermomechanical degraded samples are higher than those after thermo-oxidative
412 degradation, since the chain scission mechanism involves the presence of lower
413 molecular weight polymeric chains. Moreover, it is interesting to note that the cold
414 crystallization event occurred during the second scan becomes well pronounced for
415 thermomechanical degraded samples after 60 min of degradation (PLA,60min,TM).
416 Thus, the increase in ΔH_{cc} values together with the decrease T_{cc} for these samples reveal
417 that a reduction of PLA molar mass due to the chain scission phenomena makes the
418 systems easier to crystallize [10].
419 Considering that one of the main disadvantages of PLA is its thermal stability, Figure 8
420 shows the weight loss (Figure 8A) and its derivative, DTG, (Figure 8B) for virgin PLA
421 and the degraded samples previously considered. TGA curves for samples degraded
422 under nitrogen atmosphere are quite similar to those obtained for virgin PLA and they
423 are not included for purpose of clarity. The characteristic temperatures $T_{5\%}$ (temperature
424 for the 5 wt.% of weight loss, which can be considered as the onset degradation
425 temperature) and T_{max} (temperature of maximum weight loss rate) are summarized in
426 Table 2 for an easier comparison of the data. As can be deduced, the characteristic
427 temperatures ($T_{5\%}$ and T_{max}) are shifted to lower values with increasing degradation time
428 from 15 to 60 min, with the lowest values for the thermomechanical degraded sample
429 (PLA,60min,TM). Compared to virgin PLA, the thermo-oxidative degradation at 200 ºC
430 produces a reduction in $T_{5\%}$ of ca. 5 and 14 ºC for 15 or 60 min of degradation;
431 however, they reach a value of 27 and 36 ºC for the thermomechanical degraded
432 samples. In addition, a rather slight decrease of T_{max} are observed, with a maximum
433 value of 14 ºC. Therefore, the chain scission, which is the mechanism responsible for
434 the thermo-oxidative and thermomechanical degradation, produces the formation of
435 low-thermal stability compounds which are eliminated at moderate or low temperature

436 [19]. Furthermore, oxidation products containing ester or carbonyl group formed during
437 these degradations (see Figure 6) which are able to accelerate the thermal instability of
438 PLA [5,16,39], producing a larger decrease in $T_{5\%}$ values and, consequently, a
439 worsening of the PLA thermal stability.

440 **4. CONCLUDING REMARKS**

441 In the current study, the influence of thermal, thermo-oxidative and thermomechanical
442 degradation conditions on dynamic oscillatory rheology, chemical structure and thermal
443 properties of PLA has been evaluated. To that end, thermomechanical degradation was
444 conducted on a mixer equipped with two counter-rotating rollers, while both thermal
445 and thermo-oxidative degradation was performed on a rheometer, by using nitrogen or
446 air, respectively, as gas.

447 Dynamic oscillatory measurements in melt state indicated that an increase in the
448 temperature or time degradation, together with the application of the mechanical stress,
449 produces a larger extent of the chain scission phenomena (which was also corroborated
450 by FTIR results), since there are not rheological evidences of the formation of long
451 chain branching/crosslinking. All degraded samples present similar mechanical
452 spectrum, which are characterized by a predominant viscous behaviour (G''>G'),
453 typical of the terminal zone reported for polymer. In addition, the complex viscosity at
454 low frequency (η_0) enables to quantify the individual contribution of temperature/time
455 degradation and mechanical stress on the PLA chain scission after degradation;
456 interestingly, the contribution of mechanical stress diminishes gradually with the
457 degradation time, being more pronounced for higher degradation temperature. Even
458 though an increase in degradation temperature brings an acceleration in chain scission
459 phenomena, nitrogen is required to prevent PLA degradation with the degradation time.

With regards to the DSC findings, the comparative study between degraded samples is not possible through the crystallinity degree (χ_c), since all of them became amorphous; however, the decrease in the glass transition (T_g) is clearly ascribed to the chain scission phenomena, and the changes in the cold crystallization (ΔH_{cc}) enthalpy and its corresponding cold crystallization (T_{cc}) temperature reveal that the chain scission makes degraded samples easier to crystallize.

Finally, the thermo-oxidative and thermomechanical degradation here applied produces a worsening of the PLA thermal stability, with lower values of the characteristic temperatures ($T_{5\%}$ and T_{max}).

5. ACKNOWLEDGEMENTS

The authors thank the Departamento de Ingeniería Química of Universidad de Huelva (Centro de Investigación en Tecnología de Productos y Procesos Químicos, Pro^{2}TecS) for providing full access to laboratory equipment.

6. REFERENCES

[1] Amaro LP, Cicogna F, Passaglia E, Morici E, Oberhauser W, Al-Malaika S, Dintcheva NT, Coiai, S. Thermo-oxidative stabilization of poly(lactic acid) with antioxidant intercalated layered double hydroxides. Polym Degrad Stab 2016;133:92-100.

[2] Signori F, Coltelli MB, Bronco S. Thermal degradation of poly(lactic acid) (PLA) and poly(butylene adipate-co-terephthalate) (PBAT) and their blends upon melt processing. Polym Degrad Stab 2009;94(1):74-82.

[3] Pantani R, De Santis R, Sorrentino A, De Maio F, Titomanlio G. Crystallization kinetics of virgin and processed poly(lactic acid). Polym Degrad Stab 2010;95(7):1148-59.

[4] Rasselet, D, Ruellan A, Guinault A, Miquelard-Garnier G, Sollogoub C, Fayolle B.

485 Oxidative degradation of polylactide (PLA) and its effects on physical and mechanical
486 properties. Eur Polym J 2014;50:109-16.
487 [5] Oliveira M, Santos E, Araújo A, Fechine GJM, Machado AV, Botelho, G. The role
488 of shear and stabilizer on PLA degradation. Polym Test 2016;51:109-16.
489 [6] Paci M, La Mantia FP. Influence of small amounts of polyvinylchloride on the
490 recycling of polyethyleneterephthalate. Polym Degrad Stab 1999;63(1):11-4.
491 [7] La Mantia FP, Botta MM, Mistretta MC, Ceraulo M, Scaffaro. Degradation of
492 polymer blends: A brief review. Polym Degrad Stab 2017 Article in Press.
493 [8] Kopinke FD, Remmler M, Mackenzie K, Moder M, Wachsen O. Thermal
494 decomposition of biodegradable polyesters.2. Poly(lactic acid). Polym Degrad Stab
495 1996;53(3):329-42.
496 [9] Lim LT, Auras M, Rubino M. Processing technologies for poly(lactic acid). Prog
497 Polym Sci 2008;33(8):820-52.
498 [10] Dintcheva NT, Al-Malaika S, Morici E, Arrigo R. Thermo-oxidative stabilization
499 of poly(lactic acid)-based nanocomposites through the incorporation of clay with in-
500 built antioxidant activity. J Appl Polym Sci 2017;134(24):44974.
501 [11] Shangguan Y, Zhang C, Xie Y, Chen R, Jin L, Zheng Q. Study on degradation and
502 crosslinking of impact polypropylene copolymer by dynamic rheological measurement.
503 Polymer 2010;51(2):500-6.
504 [12] Hussein IA, Ho K, Goyal SK, Karbashewski E, Williams MC. Thermomechanical
505 degradation in the preparation of polyethylene blends. Polym Degrad Stab
506 2000;68(3):381–92.
507 [13] Drozdov AD. The effect of thermal oxidative degradation of polymers on their
508 viscoelastic response. Int J Eng Sci 2007; 45(11):882–904.
509 [14] Hussein IA. Rheological investigation of the influence of molecular structure on

510 natural and accelerated UV degradation of linear low density polyethylene. Polym
511 Degrad Stab 2007;92(11):2026-32.
512 [15] Rolón-Garrido VH, Wagner MH. Linear and non-linear rheological
513 characterization of photo-oxidative degraded LDPE. Polym Degrad Stab
514 2014;99(1):136-45.
515 [16] Amorin NSQS, Rosa G, Alves JF, Gonzalves SPC, Franchetti SMM, Fechine GJM.
516 Study of thermodegradation and thermostabilization of poly(lactide acid) using
517 subsequent extrusion cycles. J Appl Polym Sci 2013;131(6):40023.
518 [17] Hatzikiriakos SG. Long chain branching and polydispersity effects on the
519 rheological properties of polyethylenes. Polym Eng Sci 2000;40(11):2279-87.
520 [18] Tian J, Yu W, Zhou C. The preparation and rheology characterization of long chain
521 branching polypropylene. Polymer 2006;47(23):7962-7969.
522 [19] Cuadri AA, Martin-Alfonso JE. The effect of thermal and thermo-oxidative
523 degradation conditions on rheological, chemical and thermal properties of HDPE.
524 Polym Degrad Stab 2017;141:11–8.
525 [20] Martín-Alfonso JE, Franco JM. Influence of polymer reprocessing cycles on the
526 microstructure and rheological behavior of polypropylene/mineral oil oleogels. Polym
527 Test 2015;45:12-9.
528 [21] Oblak PO, González-Gutierrez J, Zupancic B, Aulova A, Emri I. Processability and
529 mechanical properties of extensively recycled high density polyethylene. Polym Degrad
530 Stab 2015;114:133-45.
531 [22] Ferry JD. Viscoelastic properties of polymers, third edition. John Wiley & Sons,
532 1980.
533 [23] Jauzein T, Huneault MA, Heuzey MC. Crystallinity and mechanical properties of
534 polylactide/ether-amide copolymer blends. J Appl Polym Sci 2017;134(4):44677.

[24] Arias A, Sojoudiasli H, Heuzey MC, Huneault MA; Wood-Adams P. Rheological study of crystallization behavior of polylactide and its flax fiber composites. J Polym Res 2017;24(3):46.

[25] Nuori S, Dubois C, Lafleur PG. Effect of chemical and physical branching on rheological behavior of polylactide. J Rheol 2015;59(4):1045-63.

[26] Singla RK, Zafar MT, Maiti SN, Ghosh AK. Physical blends of PLA with high vinyl acetate containing EVA and their rheological, thermo-mechanical and morphological responses. Polym Test 2017;63:398-406.

[27] Othman N, Acosta-Ramírez A, Mehrkhodavandi P, Dorgan JR, Hatzikiriakos SG. Solution and melt viscoelastic properties of controlled microstructure poly(lactide). J Rheol 2011;55:987-1005.

[28] Wang J, Bai J, Zhang Y, Fang H, Wang Z. Shear-induced enhancements of crystallization kinetics and morphological transformation for long chain branched polylactides with different branching degrees. Sci Rep-UK 2016;6:26560.

[29] Partal P, Martínez-Boza F, Conde B, Gallegos C. Rheological characterisation of synthetic binders and unmodified bitumens. Fuel 1999;78:1-10.

[30] Al-Itry R, Lamnawar K, Maazouz A. Improvement of thermal stability, rheological and mechanical properties of PLA, PBTA and their blends by reactive extrusion with functionalized epoxy. Poly Degrad Stab 2012;97:1898-1914.

[31] McNeill IC, Leiper HA. Degradation studies of some polyesters and polycarbonates.2. Polylactide-degradation under isothermal conditions, thermal-degradation mechanism and photolysis of the polymer. Polym Degrad. Stab 1985;11(4):309-26.

[32] Badia JD, Strömberg E, Karlsson S, Ribes-Greus A. Material valorisation of amorphous polylactide. Influence of thermos-mechanical degradation on the

560 morphology, segmental dynamics, thermal and mechanical performance. Polym Degrad.
561 Stab 2012;97(4):670-78.
562 [33] Gardette M, Thérias S, Gardette JL, Murariu M, Dubois P. Photooxidation of
563 polylactide/calcium sulphate composites. Polym. Degrad. Stab. 2011;96(4):616-23.
564 [34] Kister G, Cassanas G, Vert M. Effects of morphology, conformation and
565 configuration on the IR and Raman spectra of various poly(lactic acid)s. Polymer
566 1998;39(2):267-73.
567 [35] Park SD, Todo M, Arakawa K, Koganemaru M. Effect of crystallinity and loading-
568 rate on mode I fracture behavior of poly(lactic acid). Polymer 2006;47(4):1357-63.
569 [36] Yasuniwa M, Tsubakihara S, Takahashi K. Crystallization behavior of poly(L-
570 lactic acid). Polymer 2006;47(21):7554-63.
571 [37] Mohapatra AK, Mohanty S, Nayak SL. Poly(lactic acid) and layered silicate
572 nanocomposites prepared by melt mixing: Thermomechanical and morphological
573 properties Polym Compos 2012;33(12):2095-104.
574 [38] Russo P, Cammarano S, Bilotti E, Peijs T, Cerruti P, Acierno DJ. Physical
575 Properties of Poly Lactic Acid/Clay Nanocomposite Films: Effect of Filler Content and
576 Annealing Treatment. J Appl Polym Sci 2014;131(2):39798.
577 [39] Fan Y, Nishida H, Shirai Y, Tokiwa T. Thermal degradation behaviour of
578 poly(lactic acid) stereocomplex. Polym Degrad Stab 2004;86(2):197-208.
579

580 **Table 1.** Thermal properties evaluated from the second heating scan of virgin PLA and
581 selected degraded samples ("T", "TO" and "TM" corresponds to thermal, thermo-
582 oxidative and thermomechanical degradation, respectively).

	T_g (ºC)	T_{cc}(ºC)	T_m or T_{m1}/T_{m2} (ºC)	ΔH_m (J/g)	ΔH_{cc} (J/g)	χ_c (%)
Virgin PLA	58.9 ± 0.5	--	[a]148.2 ± 0.3	[a]31.9 ± 1.3	--	[a]34.3 ± 1.5
PLA,15min,T	59.1 ± 0.5	135.1 ± 0.5	148.7 ± 0.3	1.9 ± 0.5	1.6 ± 0.5	[b]Amorphous
PLA,60min,T	59.3 ± 0.5	135.5 ± 0.5	148.9 ± 0.3	1.8 ± 0.6	1.7 ± 0.5	[b]Amorphous
PLA,15min,TO	49.7 ± 0.5	124.5 ± 0.6	144.5/150.2 ± 0.4	5.5 ± 1.0	5.2 ± 1.1	[b]Amorphous
PLA,60min,TO	50.6 ± 0.5	124.8 ± 0.6	144.7/150.4 ± 0.4	5.9 ± 1.0	5.4 ± 1.2	[b]Amorphous
PLA,15min,TM	51.2 ± 0.6	120.8 ± 0.6	147.2/153.0 ± 0.4	17.1 ± 1.2	16.6 ± 1.4	[b]Amorphous
PLA,60min,TM	52.0 ± 0.6	122.1 ± 0.6	147.3/153.5 ± 0.4	21.4 ± 1.2	21.2 ± 1.5	[b]Amorphous

583 [a] Evaluated form the first heating scan.
584 [b] Amorphous; calculated crystallinity degree is about zero, i.e., less than 1 %.
585

586 **Table 2.** Thermal degradation characteristic temperatures of virgin PLA and selected
587 degraded samples ("T", "TO" and "TM" corresponds to thermal, thermo-oxidative and
588 thermomechanical degradation, respectively).

	$T_{5\%}$ (ºC)	T_{max} (ºC)
Virgin PLA	322.4 ± 1.0	367.1 ± 1.0
PLA,15min,T	322.0 ± 1.0	366.7 ± 1.0
PLA,60min,T	321.7 ± 1.0	366.6 ± 1.3
PLA,15min,TO	317.9 ± 1.1	361.1 ± 1.2
PLA,60min,TO	308.8 ± 1.1	357.2 ± 1.2
PLA,15min,TM	295.7 ± 1.2	357.4 ± 1.2
PLA,60min,TM	286.1 ± 1.2	353.1 ± 1.2

589

590

591 **Figure captions**

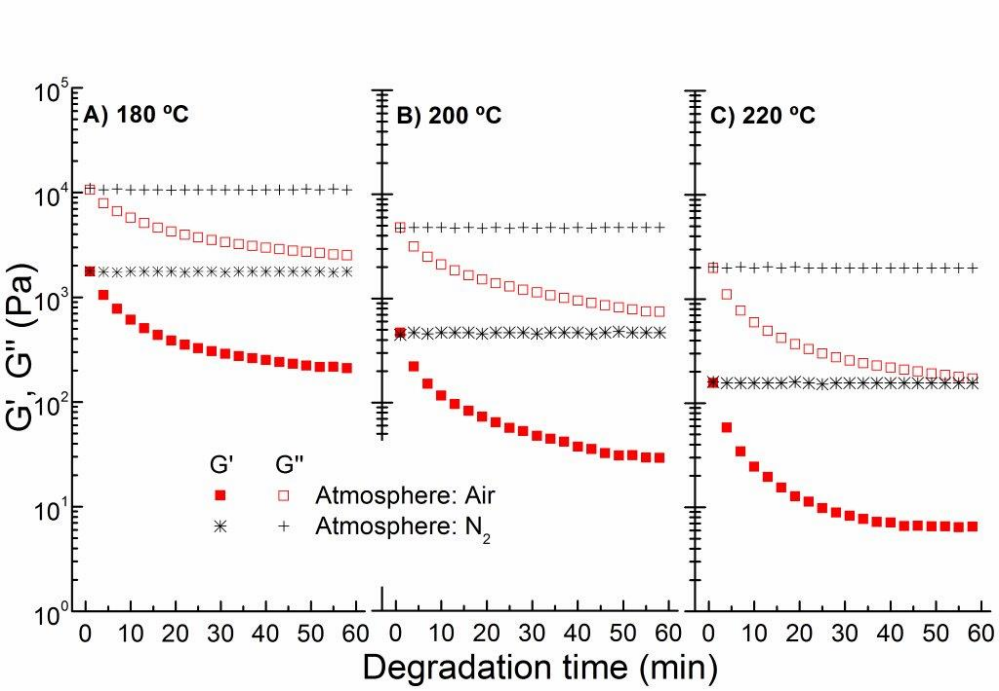

592

593 **Figure 1.** Evolution of the storage (G') and loss (G'') modulus with the degradation

594 time for samples subjected to different degradation conditions.

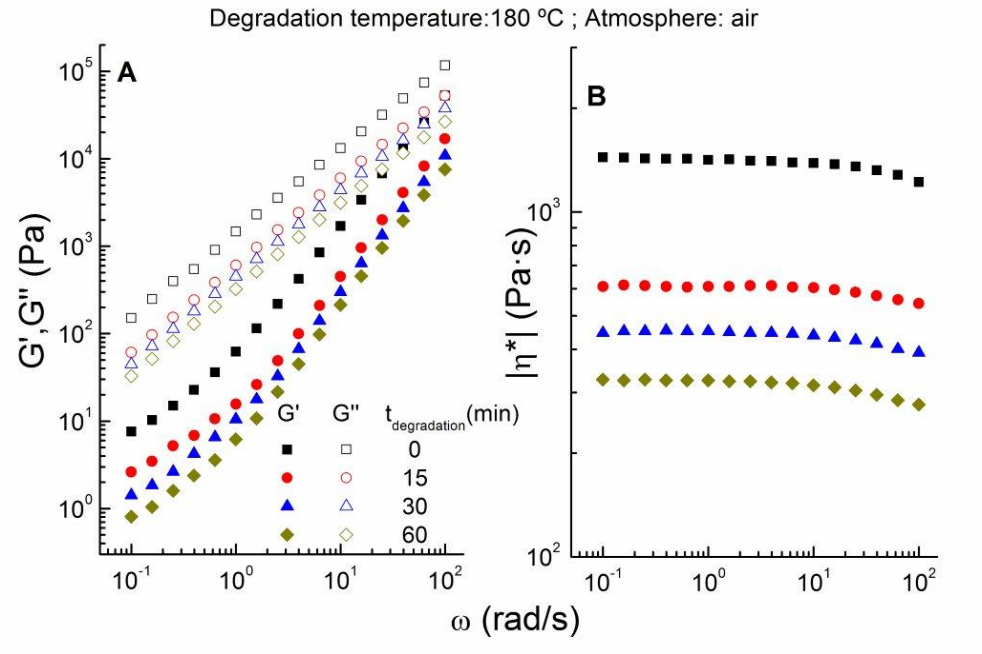

595

596 **Figure 2.** Evolution of (A) the storage (G') and loss (G'') modulus, and (B) complex
597 viscosity with frequency for degraded samples under air atmosphere at 180 ºC, as a
598 function of degradation time.

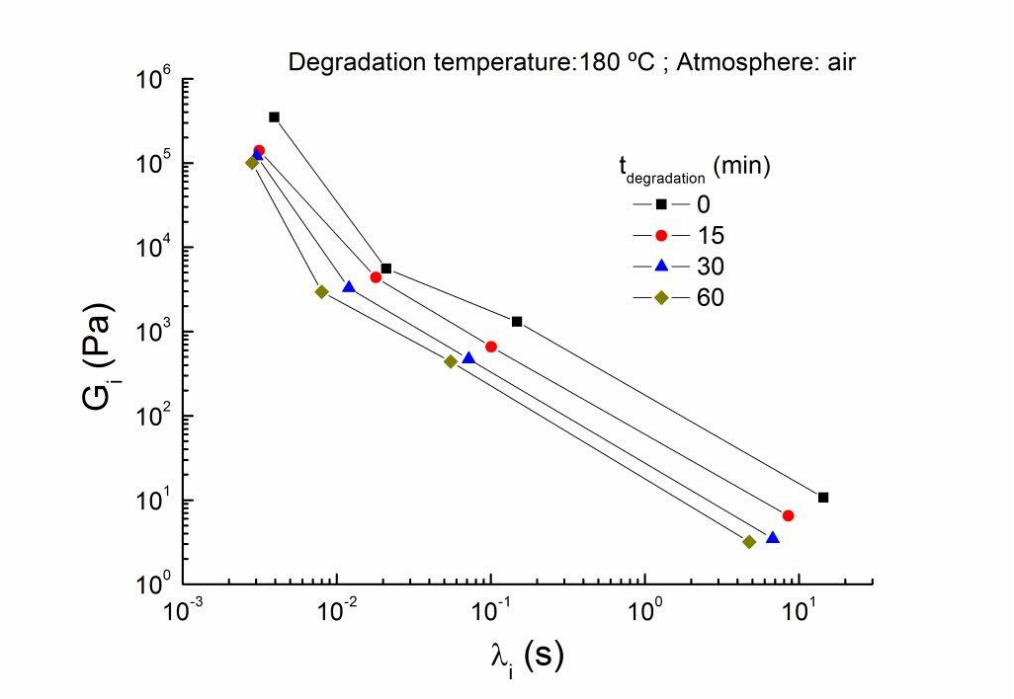

599

600 **Figure 3**. Discrete relaxation spectra for degraded samples under air atmosphere at 180
601 ºC, as a function of degradation time.

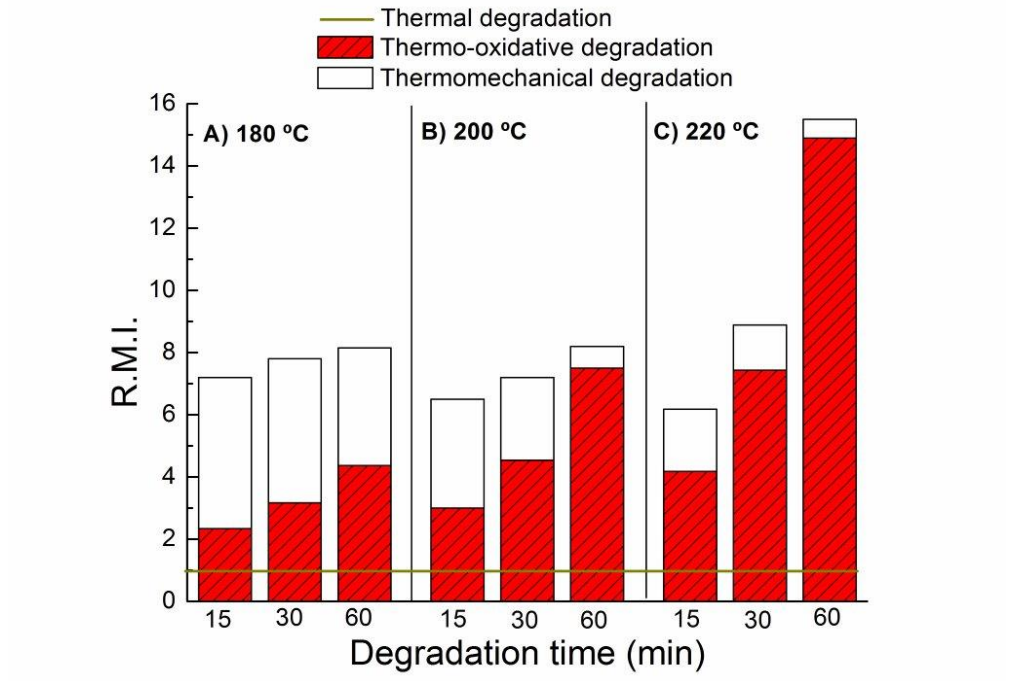

602

603 **Figure 4.** Evolution of relative modification index (R.M.I.) with the degradation time
604 for samples subjected to different degradation conditions.

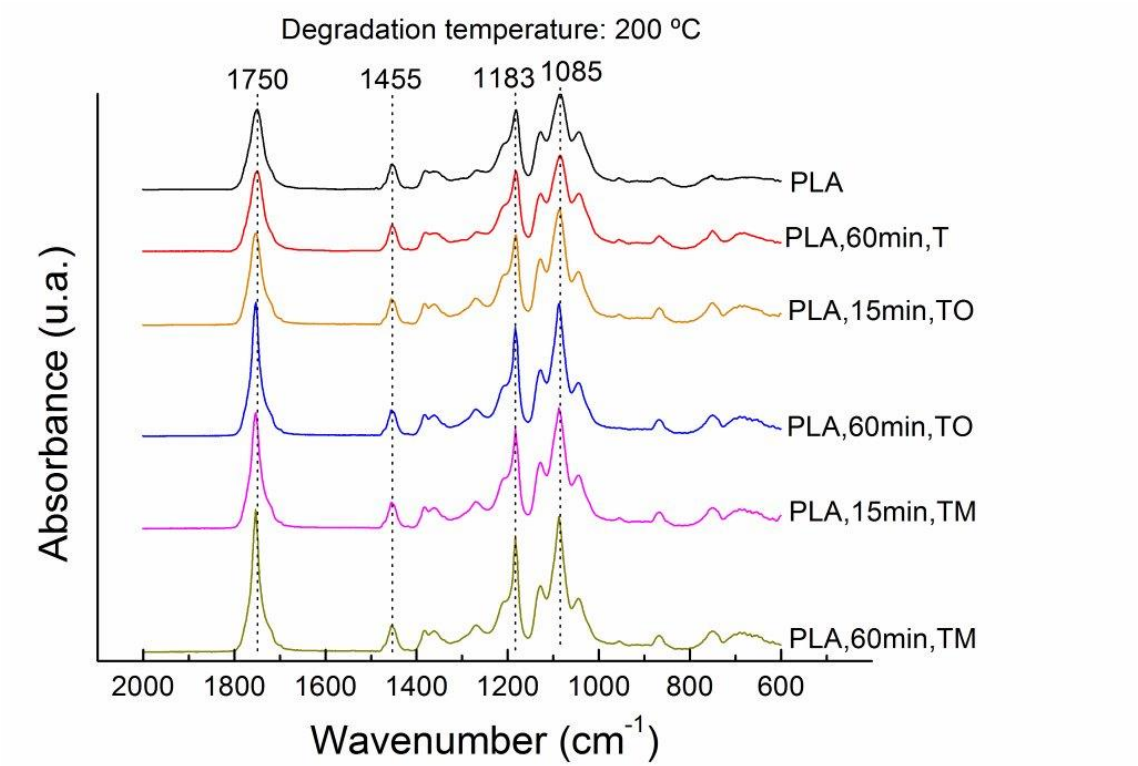

605

606 **Figure 5.** ATR-FTIR spectra for virgin PLA and selected degraded samples subjected
607 to different degradation conditions ("T", "TO" and "TM" corresponds to thermal,
608 thermo-oxidative and thermomechanical degradation, respectively).

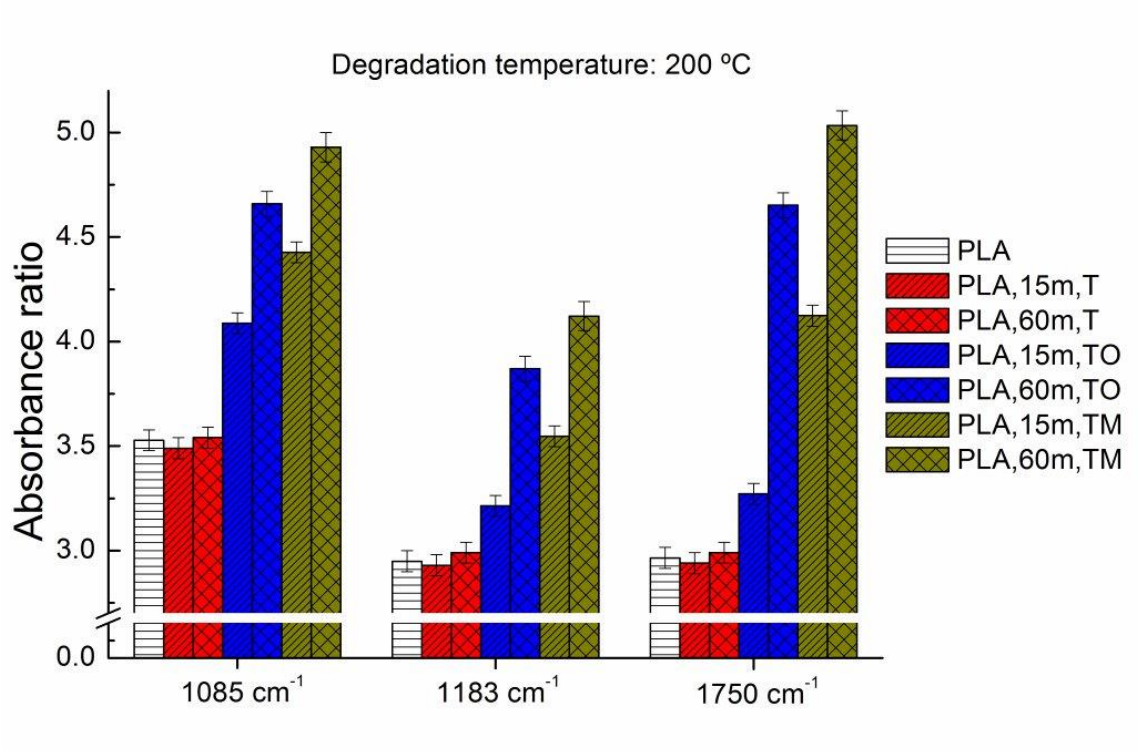

609

610 **Figure 6.** Absorbance ratio for the peak at 1085, 1183 and 1750 cm^{-1} for virgin PLA
611 and selected degraded samples subjected to different degradation conditions ("T", "TO"
612 and "TM" corresponds to thermal, thermo-oxidative and thermomechanical degradation,
613 respectively).

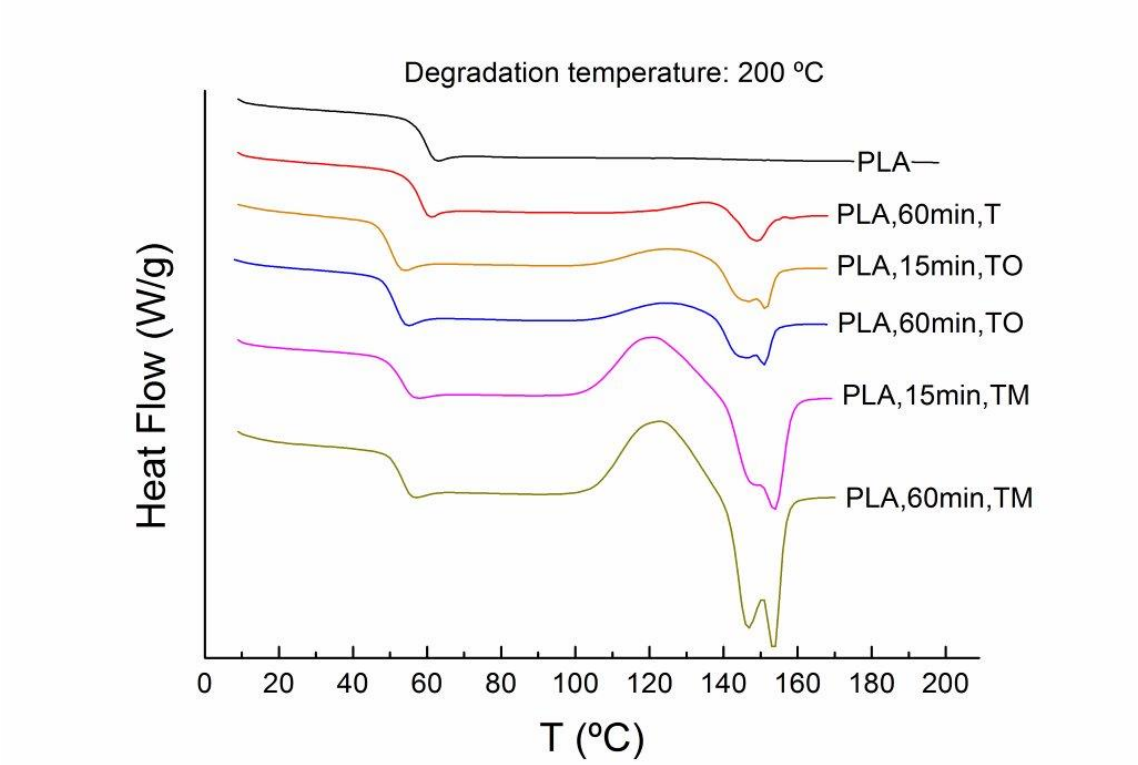

614

615 **Figure 7.** DSC curves corresponding to the second heating cycle for the virgin PLA and
616 selected degraded samples subjected to different degradation conditions ("T", "TO" and
617 "TM" corresponds to thermal, thermo-oxidative and thermomechanical degradation,
618 respectively).

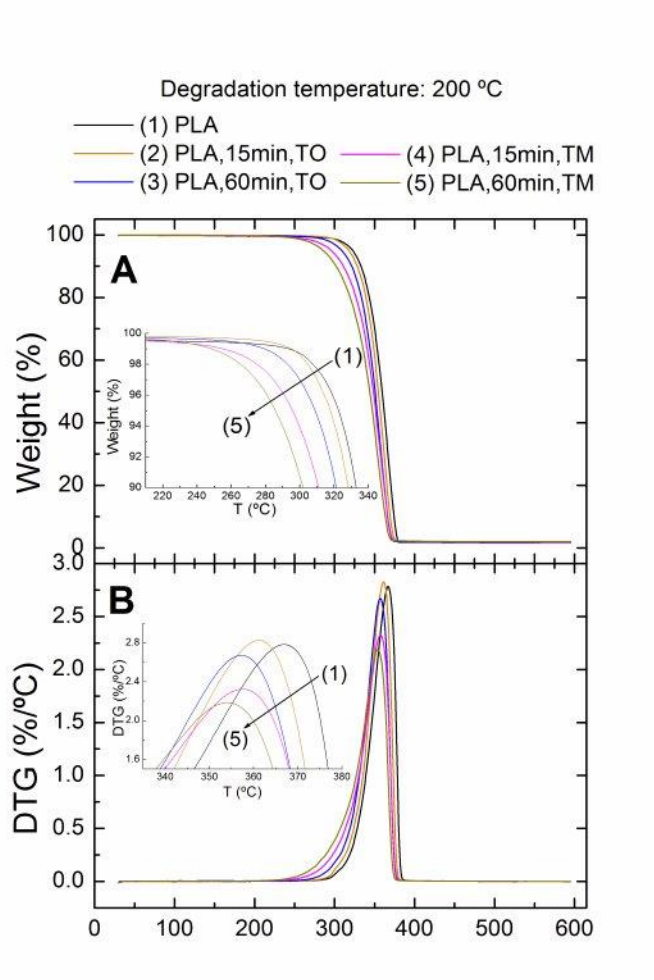

619

620 **Figure 8.** (A) Weight loss and (B) its derivative curves for the virgin PLA and selected
621 degraded samples subjected to different degradation conditions ("T", "TO" and "TM"
622 corresponds to thermal, thermo-oxidative and thermomechanical degradation,
623 respectively).